Reprinted from June 1991, Vol. 113, Journal of Applied Mechanics

Chaotic Motions of a Constrained Pipe Conveying Fluid: Comparison Between Simulation, Analysis, and Experiment

M. P. Paidoussis
Fellow ASME

G. X. Li

Department of Mechanical Engineering,
McGill University,
Montreal, QC H3A 2K6, Canada

R. H. Rand
Department of Theoretical and Applied Mechanics,
Cornell University,
Ithaca, NY 14853

A refined analytical model is presented for the dynamics of a cantilevered pipe conveying fluid and constrained by motion limiting restraints. Calculations with the discretized form of this model with a progressively increasing number of degrees of freedom, N, *show that convergence is achieved with* N = *4 or 5, which agrees with previously performed fractal dimension calculations of experimental data. Theory shows that, beyond the Hopf bifurcation, as the flow is increased, a pitchfork bifurcation is followed by a cascade of period doubling bifurcations leading to chaos, which is in qualitative agreement with observation. The numerically computed theoretical critical flow velocities are in excellent quantitative agreement (5–10 percent) with experimental values for the thresholds of the Hopf and period doubling bifurcations and for the onset of chaos. An approximation for the critical flow velocity for the loss of stability of the post-Hopf limit cycle is also obtained by using center manifold concepts and normal form techniques for a simplified version of the analytical model; it is found that the values obtained in this manner are approximately within 10 percent of those computed numerically.*

1 Introduction

The linear and nonlinear dynamics of cantilevered pipes conveying fluid has been studied quite extensively, both theoretically and experimentally. Indeed, this system has become a paradigm in the study of stability nonconservative circulatory systems (Païdoussis, 1987; Païdoussis and Issid, 1974; Holmes, 1977). More recently, variants of this system have been shown to exhibit complex dynamics and chaos, as described below.

Tang and Dowell (1988) have used a pipe with an inset steel strip and equispaced magnets on either side, buckling the pipe into one or the other potential well thus generated. Once the flow velocity is sufficiently above the threshold value for flutter about the buckled state, chaotic oscillations were shown to be possible. This problem was studied theoretically, while its nonautonomous counterpart (forced vibration) was studied both theoretically and experimentally, once again displaying chaos. The theoretical results were in encouragingly good agreement with experimental observations.

Païdoussis and Moon (1988) studied the dynamics of a cantilevered pipe constrained by nonlinear motion restraints. For flow velocities sufficiently higher than the critical for the Hopf bifurcation, the limit cycle motion was large enough for the pipe to impact on the restraints; as the flow was incremented further, a series of period doubling bifurcations led to chaos. The special merit of this study is that it was the first joint experimental/theoretical one involving chaos in an *autonomous mechanical system* (Moon, 1987). This system was studied more fully on the theoretical side by Païdoussis, Li, and Moon (1989).

The analytical model utilized in the foregoing studies was four-dimensional (two degrees-of-freedom), which is the minimum possible for chaos in this autonomous system. Analysis of typical experimental vibration signals yielded a fractal dimension of 3.2 in the chaotic regime (Païdoussis, Cusumano, and Copeland, 1991), suggesting that although four-dimensional modeling may be reasonable, eight or ten-dimensional models may be necessary to capture all essential features of the dynamics. Indeed, although experiment and four-dimensional simulation in that study displayed remarkable qualitative similitude, quantitative agreement, although reasonable, was not good—e.g., for the threshold flow velocities for period doubling or chaos. Moreover, it was not known if the four-dimensional results were representative of those of higher-

Contributed by the Applied Mechanics Division of THE AMERICAN SOCIETY OF MECHANICAL ENGINEERS for presentation at the Joint Applied Mechanics/Bioengineering Conference, Ohio State University, Columbus, OH, June 16–19, 1991.

Discussion on this paper should be addressed to the Technical Editor, Leon M. Keer, The Technological Institute, Northwestern University, Evanston, IL 60208, and will be accepted until two months after final publication of the paper itself in the JOURNAL OF APPLIED MECHANICS. Manuscript received by the ASME Applied Mechanics Division, Nov. 21, 1989; final revision, Oct. 2, 1990.

Paper No. 91-APM-36.

dimensional models in quantitative terms; thus, whether the agreement found was fortuitous or not.

In the present paper, a systematic *quantitative* comparison between experiment and theory is undertaken, considering progressively higher-dimensional models, while at the same time refining the analytical model to bring it closer to experimental reality. Moreover, the first post-Hopf bifurcation in the four-dimensional system is predicted by analytically reducing the problem to a two-dimensional system through center manifold analysis, thus permitting a three-cornered overall comparison between experiment, simulation, and analysis.

In physical terms, this system is an example of a large class of problems involving self-excited oscillations and interactions with motion limiting constraints. An example is the so-called fluid-elastic oscillation of heat exchanger tubes impacting on the generally loosely fitting baffle plates (Axisa et al., 1988), leading to chaotic-looking oscillations and resulting in potentially catastrophic wear rates for the tubes. Hence, understanding and modeling the dynamics of such systems is of both fundamental and practical interest.

2 The Experiments

Although the experimental apparatus, measurements, and data analysis are described fully elsewhere (Païdoussis and Moon, 1988), a few words here will nevertheless be useful. Fig. 1(*a*, *b*) shows the most successful version of the experimental apparatus. It consisted of a vertical cantilevered pipe made of elastomer, containing water flowing downwards. An embedded thin metal-strip-enforced planar motions. The post-Hopf limit cycle amplitude was constrained by motion limiting restraints, typically two polycarbonate bars, Fig. 1(*b*).

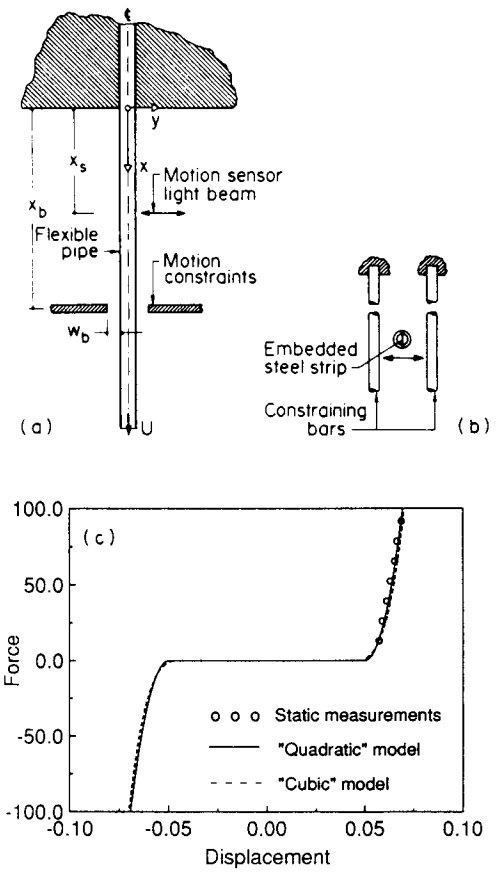

Fig. 1(*a*) Schematic of the experimental system; (*b*) scheme for achieving planar motions with steel strip embedded in the pipe, also showing motion constraining bars; (*c*) modeling of restraint stiffness, also showing static force-displacement measurements

Motion of the system was measured with the aid of a non-contacting optical tracking system. The signal was processed through a FFT Analyzer and a digital storage oscilloscope, yielding power spectra (PSD), phase plane plots, probability density (PDF), and autocorrelation functions, while the flow velocity was incremented.

Typically, experiments showed that as U was increased beyond the Hopf bifurcation, regular motion (involving impacting with one or both constraining bars in each cycle of motion) was succeeded by period-2 motion (with impacting once every two cycles). More irregular motion developed at higher U; with the help of experimental PSD, PDF, and autocorrelation function plots and Poincaré maps, it was conclusively shown that the oscillations, beyond a certain U, became chaotic. Thus, the critical flow velocities for the Hopf and period doubling bifurcations and for the onset of chaos were determined experimentally.

3 The Equation of Motion

3.1 The Basic Model. The equation of motion of a vertical cantilevered pipe conveying fluid (Païdoussis, 1970) was modified to take into account the presence of motion limiting restraints (Païdoussis et al., 1989). For a pipe of flexural rigidity EI, coefficient of Kelvin-Voigt viscoelastic damping a, length L and mass-per-unit-length m, conveying fluid of mass-per-unit-length M with velocity U, subject to planar motions $w(x,t)$ and impacting with nonlinear force $F(w)$ on the restraint, Fig. 1, the nondimensional equation of motion is given by

$$\left(1+\alpha\frac{\partial}{\partial\tau}\right)\frac{\partial^4\eta}{\partial\xi^4}+[u^2-\gamma(1-\xi)]\frac{\partial^2\eta}{\partial\xi^2}+2\beta^{1/2}u\frac{\partial^2\eta}{\partial\xi\partial\tau}+\gamma\frac{\partial\eta}{\partial\xi}+f(\eta)\delta(\xi-\xi_b)+\frac{\partial^2\eta}{\partial\tau^2}=0, \quad (1)$$

where $\eta=w/L$, $\xi=x/L$, $\tau=[EI/(M+m)]^{1/2}t/L^2$, t denoting time, $u=(M/EI)^{1/2}UL$, $\beta=M/(M+m)$, $\gamma=(M+m)gL^3/EI$, $\alpha=[EI/(M+m)]^{1/2}a/L^2$, $f(\eta)=F(w)L^3/EI$, and $\delta(x-x_b)$ is the Dirac delta function. This equation holds for a sufficiently long and slender pipe, where the Euler-Bernoulli beam theory is appropriate, and for small pipe deflections, imposed by the motion restraints, where the motion may adequately be described by a linearized equation (apart from interaction with the nonlinear restraints). It is recalled that the problem is independent of fluid frictional effects (Gregory and Païdoussis, 1966), which are therefore absent from equation (1).

3.2 The Adapted Model. Some aspects of the model, e.g., the stiffness of the restraining bars, Fig. 1(*b*), and the damping characteristics of the pipe, need to be adapted to the particular system being modeled, since direct quantitative comparison to the experimental results will be made. The experimental system, for which the most extensive and reliable set of data was available, was selected (Païdoussis and Moon, 1988; pipe no. 9, Fig. 6). The nondimensional parameters for this system are as follows: $\beta=0.213$, $\gamma=26.76$, $\xi_b=0.65$; the dimensionless gap to the restraints (Fig. 1(*a*)), $\eta_b=w_b/L=0.055$.

The damping characteristics of the empty, silicone rubber vertical pipe were measured with the aid of an FFT Analyzer and Hilbert transform techniques. The logarithmic decrements of the lowest three modes were $\delta_1=0.028$, $\delta_2=0.081$, and $\delta_3=0.144$. This suggests that damping was viscohysteretic, rather than purely viscoelastic. In what follows, it was found convenient to utilize a modal damping representation; thus, for the rth mode, the damping term in equation (1) was modified:

$$\alpha\frac{\partial^5\eta}{\partial\tau\partial\xi^4}\to c_r\frac{\partial\eta}{\partial\tau}\equiv\frac{\delta_r\omega_r}{\pi}\frac{\partial\eta}{\partial\tau}, \quad (2)$$

where ω_r are the zero-flow dimensionless eigenfrequencies of the vertical pipe. As the measured δ_r vary almost linearly with r and reliable measurement of δ_r for $r>3$ was found impossible, and higher δ_r were linearly extrapolated when required.

In previous work (e.g., Païdoussis et al., 1989) the restraining force was modeled by a cubic spring, $f(\eta)=\kappa\eta^3$, which represents a compromise: although this form of $f(\eta)$ is mathematically convenient, it does not model the physical situation perfectly, since it does not recognize that in the free gap the constraint is zero, rather than just small. The stiffness of the restraining bars, Fig. 1(*b*), was determined by applying static loads and measuring the resulting deflection; the results are shown in Fig. 1(*c*). The stiffness is slightly hardening, but almost linear, suggesting something close to trilinear modeling (Moon and Li, 1990): $f(\eta)=\kappa\{\eta-1/2(|\eta+\eta_b|-|\eta-\eta_b|)\}$, which yields $\kappa(\eta-\eta_b)$ for $\eta\geq\eta_b$, $\kappa(\eta+\eta_b)$ for $\eta\leq-\eta_b$ and 0 for $|\eta|<|\eta_b|$. However, the appropriateness of a trilinear model for representing dynamical impact (Hunt and Crossley, 1975), especially in view of the pipe itself being flexible, was questioned: in particular, the abrupt application of the total force of the restraint (abrupt change in slope in Fig. 1(*c*)) at $|\eta|=|\eta_b|$. The following three adaptations to the trilinear model were therefore adopted instead:

$$f(\eta)=\kappa_n\left\{\eta-\frac{1}{2}(|\eta+\eta_{bn}|-|\eta-\eta_{bn}|)\right\}^n,\quad n=2,3,5, \tag{3}$$

in which the sharp discontinuity at $|\eta|=|\eta_b|$ is smoothed; least squares fitting gave the following set of values: for $n=2$, $\kappa_2=2.7\times10^5$, $\eta_{b2}=0.050$, for $n=3$, $\kappa_3=5.6\times10^6$, $\eta_{b3}=0.044$; for $n=5$, $\kappa_5=1.0\times10^9$, $\eta_{b5}=0.031$. These models will henceforth be referred to as "quadratic," "cubic," and "quintic" for short; in the quadratic, clearly $(\eta-\eta_b)^2=(\eta-\eta_b)|\eta-\eta_b|$ to preserve functional oddness. The resulting approximations to the dynamical restraint stiffness are shown in Fig. 1(*c*) for $n=2$ and 3; the curve for $n=5$ is very close to those shown but is omitted to preserve clarity. Calculations will be conducted with all three restraint models and the results compared.

4 Low-Dimensional Models and Convergence

In view of the results of fractal dimensional calculations, the infinite dimensional model will be discretized, and the dynamics of the resultant low-dimensional models, represented by a set of ordinary differential equations, will be explored and later compared to experiment.

4.1 The Reduction Procedure. The system is discretized by utilizing the standard Galerkin expansion

$$\eta(\xi,\tau)=\sum_i\phi_i(\xi)q_i(\tau), \tag{4}$$

where the $\phi_i(\xi)$ chosen are the dimensionless orthonormal set of cantilever beam eigenfunctions. Upon substituting (4) into equation (1), with (2) taken into account, multiplying by $\phi_j(\xi)$ and integrating over the domain (0,1), one obtains

$$\{\ddot{q}\}+[C]\{\dot{q}\}+[K]\{q\}+\{f(q)\}=0, \tag{5}$$

where the elements of the matrices are given in Païdoussis et al. (1989). For purposes of numerical simulation, equation (5) should further be reduced to first-order form:

$$\{\dot{q}\}=\{p\},\quad \{\dot{p}\}=-[C]\{p\}-[K]\{q\}-\{f(q)\}, \tag{6}$$

where $\{q\}$ and $\{p\}$ are the generalized displacement and velocity vectors. If the summation in (4) is truncated at $i=N$, an N degree-of-freedom, i.e., a $2N$-dimensional model of the continuous system is generated.

Once $\{p\}$ and $\{q\}$ are determined, the deflection of the pipe and its velocity at any point ξ may be expressed approximately as

$$\eta(\xi,\tau)\simeq\sum_{i=1}^{N}\phi_i(\xi)q_i(\tau),\ \dot{\eta}(\xi,\tau)\simeq\sum_{i=1}^{N}\phi_i(\xi)p_i(\tau). \tag{7}$$

4.2 The Hopf Bifurcation. All system parameters are fixed as defined in Section 3.2 and the dimensionless flow velocity u is gradually increased. Eventually, for high enough u the hitherto stable equilibrium is lost, giving birth (if nonlinearities are taken into account) to a stable limit cycle. This defines a Hopf bifurcation, which corresponds to single-degree-of-freedom flutter in aeroelastic terminology. The critical value of $u=u_H$ for the Hopf bifurcation may be found by solving the eigenvalue problem of the linearized system (6); it occurs once two complex conjugate eigenvalues with hitherto negative real parts become purely imaginary and then cross to the positive side of the λ-plane.

The main concern here is the number of modes necessary for accurate prediction of the Hopf bifurcation. The results are shown in Fig. 2. It is seen that convergence is effectively achieved with $N=4$ (c.f., Païdoussis, 1970). The $N=2$ model used in the previous studies of this problem underestimates u_H by 14 percent.

4.3 Period Doubling Bifurcations and Chaos. It has been shown previously for an $N=2$ (four-dimensional) system (Païdoussis and Moon, 1988; Païdoussis et al., 1989) that for u sufficiently above u_H, the stability of the limit cycle is destroyed by a transcritical-like pitchfork bifurcation (destroying the symmetry of the limit cycle), followed at higher u by a period doubling bifurcation; as u is increased further, a cascade of period doubling bifurcations leads to chaos. Of interest here is (i) to explore higher-dimensional ($N>2$) model behavior and possible convergence of the results with N, (ii) to do simulations with the refined analytical model for precise values of the parameters applicable to the experimental system. It is important to recall that in all the foregoing simulations with $N=2$ it was possible to conduct calculations only with $\xi_b\geq0.75$, instead of the actual $\xi_b=0.65$; furthermore, diminished values of the stiffness of the cubic spring (used to model restraint stiffness in the earlier studies) had to be used. Both limitations were imposed by failure of the solution to converge otherwise; more specifically, the solution trajectory tended to escape to infinity, no matter how small the integration step size, the reasons for which have not yet been elucidated.

The simulations were done by integrating equations (6) by the standard fourth-order Runge-Kutta algorithm. The parameter varied is u, whilst the output utilized to display bifurcations is the approximate free-tip velocity of the pipe $\dot{\eta}(1,\tau)$, equations (7). The triggering signal is $\eta(1,\tau)$: when $\eta(1,\tau)=0$ and $\dot{\eta}(1,\tau)>0$, the value of $\dot{\eta}(1,\tau)$ is recorded.

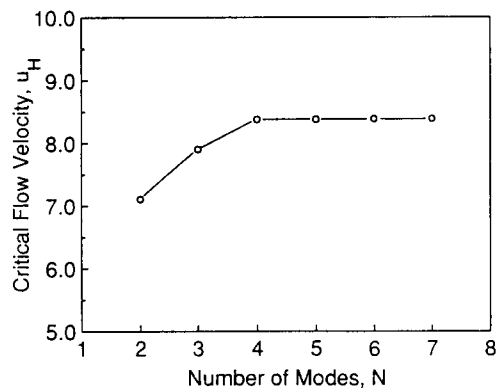

Fig. 2 Convergence of the critical flow velocity for the Hopf bifurcation as a function of the number of modes, *N*, in the Galerkin discretization

The first thing to remark is that no difficulty was encountered in the simulations for $N>2$ in obtaining convergent solutions for the experimental set of parameters chosen in Section 3.2. Hence, the difficulties referred to in the foregoing must have been related to the inability of the $N=2$ model to properly model the experimental system.

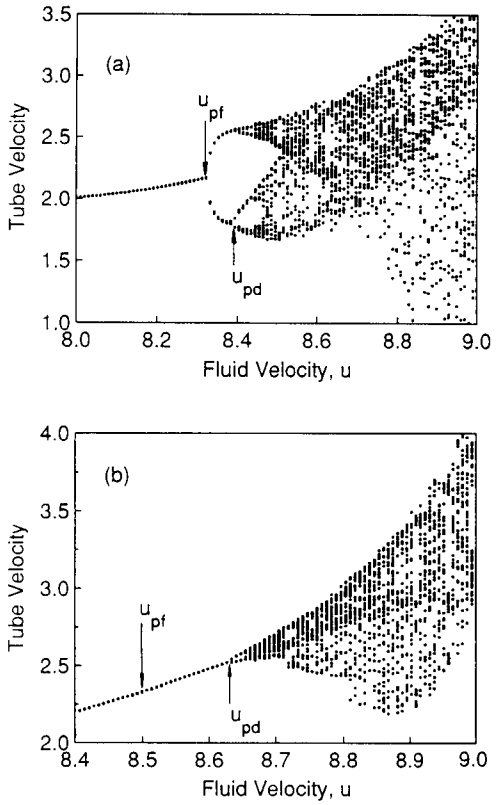

Fig. 3 Bifurcation diagram showing the tube-tip dimensionless velocity amplitude with the dimensionless fluid velocity u as the bifurcation parameter, utilizing the quadratic restraint stiffness representation for *(a)* $N=3$ and *(b)* $N=5$. The subscripts *pf* and *pd*, respectively, refer to pitchfork and period doubling bifurcations

Bifurcation diagrams were constructed for $N=3$ to 7, i.e., six-dimensional to fourteen dimensional systems, for each of three representations of the restraint stiffness, equation (3). Typical results are shown in Fig. 3 for the quadratic model ($n=2$ in equation (3), see also Fig. 1(*b*)) for $N=3$ and $N=5$. Only the portion beyond the Hopf bifurcation is shown in Fig. 3.

In Fig. 3(*a*) it is clearly seen that the first post-Hopf bifurcation occurs at $u=8.325$, followed by another one at $u=8.357$. By referring to Fig. 4(*a*), it is seen that the former is a transcritical-like pitchfork bifurcation, whereby the symmetry of the orbit has been destroyed;[1] the two branches of the pitchfork in Fig. 3(*a*) are obtained with opposite-sign initial conditions. The second bifurcation shown (Fig. 3(*a*), $u=8.357$) is a period doubling one, followed by a cascade of further such bifurcations leading to chaos—a common route to chaos for many continuous systems (Tousi and Bajaj, 1985; Moon, 1988). Figure 4(*b*) shows period-4 motion, while Fig. 4(*c,d*) strongly chaotic motion. In the spectrum of Fig. 4(*d*), the principal frequency peak is only 25 dB approximately above the broadband component of the signal, whereas for weakly chaotic motion at a lower velocity ($u=8.5$, not shown), this peak is prominently above (by 40 dB) the broadband component.

Figure 3(*b*) displays bifurcations for the $N=5$ model, of the same type as for the $N=3$ model of Fig. 3(*a*), but at somewhat different values of u and with some other qualitative differences. Thus, the first period doubling bifurcation occurs at $u=8.630$, as compared to 8.357, which nevertheless are only three percent apart. Also, the pitchfork bifurcation, which is very prominent in Fig. 3(*a*), is just discernible in Fig. 3(*b*).

The bifurcation diagrams with the cubic and quintic representation of the restraint stiffness are quite similar to those of Fig. 3, and are not presented for brevity.

As a measure of convergence of these results, as N is increased and as the model of the restraint stiffness is varied, the first period doubling bifurcation threshold was chosen.

[1] It is recalled that the phase-plane plots are in terms of approximate tip displacement and velocity, equations (7), whereby the $2N$-dimensional space is recomposed into a two-dimensional projection.

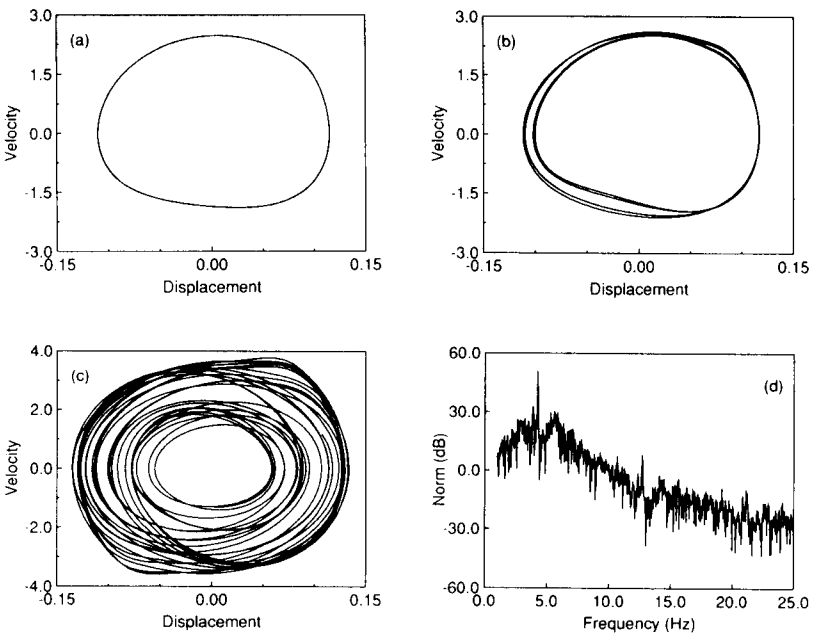

Fig. 4 Phase plane diagrams of tube-tip velocity $\dot{\eta}(1,\tau)$ versus tube-tip displacement, $\eta(1,\tau)$, obtained with $n=2$ and $N=3$; c.f., Fig. 3(*a*), for *(a)* $u=8.35$, *(b)* $u=8.445$, *(c)* $u=9.00$, *(d)* the corresponding power spectrum for $u=9.00$

The results are shown in Fig. 5. It is seen that for $N=5$ each of the three curves has converged to a steady value. It should be noted that, although looking relatively distant from one another, the three values of the threshold flow velocity for period doubling, u_{pd}, differ by less than 3.5 percent for $N \geq 5$; hence, any one of the three restraint stiffness representations is as good as any of the others, although perhaps the quadratic, which matches closest the data of Fig. 1(*c*)—cf., equation (3), $n=2$—may be considered to be the "best."

Before leaving this section, it should be mentioned that in all simulations, the initial conditions were fixed: $q_1(0) = \pm 0.05$, $q_i(0) = 0$ for $i = 2, \ldots, N$, and $p_i(0) = 0$ for $i = 1,2, \ldots, N$, where the $\pm$ values were used to obtain the two branches after the pitchfork bifurcation, Fig. 3. Other initial conditions were tried, but the system was found to be insensitive to the specific choice made, provided that the values were not too large; if they were, then, in some parameter ranges, the numerical solutions "blew up."

5 Comparison of Theoretical to Experimental Results

The results of the analytical model proposed here, encompassing a more realistic representation of the physical system, are qualitatively similar to those of the more idealized versions of the analytical model utilized heretofore (see Païdoussis et al., 1989, 1991), which were already shown to be *qualitatively* similar to those of the experimental system. Accordingly, it is not necessary to undertake a qualitative comparison here. Suffice it to say that the dynamical behavior in terms of the route to chaos and general dynamical character of the motion, as seen in phase plane plots, power spectra, and autocorrelations of the experimental system, is remarkably similar. Nevertheless, it must be stressed that the theoretical results here are the first ever to be presented (and possible) with all system parameters closely matching the experimental system.

In this section the crucial *quantitative* comparison between theory and experiment will be undertaken. In this regard, it is noted that the results of the analytical model have been shown to be convergent (Section 4.3), so that possible agreement with experiment cannot be spurious. The comparison is undertaken in terms of the threshold u for the Hopf and first period-doubling bifurcations, u_H and u_{pd}, and for chaos, u_{ch}. The experimental values have been obtained from Païdoussis and Moon's work (Fig. 6 of that paper).

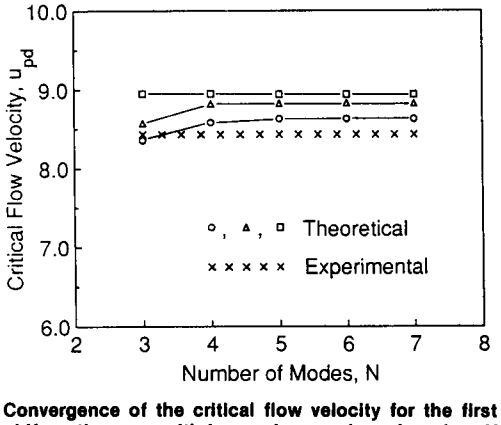

Fig. 5 Convergence of the critical flow velocity for the first period-doubling bifurcation, u_{pd}, with increasing number of modes, N, for the three representations of restraint stiffness: quadratic (○), cubic (▵) and quintic (□); also, shown is the experimental result (× ×)

The experimental value of u_{pd} may be compared to theoretical ones in Fig. 5. Numerical values are compared in Table 1. The uncertainty in the experimental results is related to the measurement of the flow velocity and other quantities entering into its nondimensionalization, and also in deciding where exactly the experimental threshold was. The theoretical range arises from the various models for restraint stiffness. The percent discrepancy between theory and experiment is of the order of 5 percent throughout; if possible uncertainties in the experimental results are taken into account, then a maximum possible discrepancy of 8–11 percent is obtained. For this type of system, such agreement between theory and experiment is deemed to be excellent.

6 Stability Analysis

In Section 4 it was seen that the transition to chaos was characterized by a series of bifurcations and associated changes in stability. The first, the Hopf bifurcation, leading to the birth of a limit cycle, has been analyzed through the linearized system. Hence, attention will be focused here on the next bifurcation, which corresponds to loss of stability of the limit cycle itself.

In this section, a stability analysis is undertaken, aimed at calculating u^*, the value of u which corresponds to change of stability of the limit cycle. The approach is based on "center manifold analysis" and follows a strategy described by Rand (1989).

The idea of center manifold analysis is to decrease the dimension of the system being studied by eliminating directions in the phase space which are unimportant for the bifurcation under consideration. This is accomplished by restricting attention to an invariant subspace (the center manifold), containing all essential behavior of the system in the neighborhood of the equilibrium point. Practical considerations dictate that this analysis, feasible in principle for any N, be limited to $N=2$, i.e., a four-dimensional system.

Thus, in system (6), the Hopf bifurcation is characterized by the appearance of two pure imaginary eigenvalues in the equations linearized about the equilibrium point at the origin. Since the other two eigenvalues have negative real parts, the motion of the linearized system will asymptotically approach the space $\mathcal{L}$ spanned by the eigenvectors corresponding to those eigenvalues with zero real parts. In the nonlinear system (6), there exists a curved subspace CM (the center manifold), tangent to the flat subspace $\mathcal{L}$ at the origin, which is invariant under the flow generated by the nonlinear equations.

In order to approximate the critical u^*, the following procedure is followed: (1) an approximation for the CM is obtained; (2) perturbations are used on the resulting two-dimensional problem in order to approximate the limit cycle; (3) the stability of the limit cycle is examined by considering only the two directions normal to the center manifold. The point of the calculation is that, although the original problem was four-dimensional, it is reduced to a two-dimensional problem.

Table 1 Comparison of theoretical to experimental values of the threshold flow velocities for the Hopf and period doubling bifurcations and for chaos. The percent difference is with respect to experiment; "maximum percent differences" represent maximum possible discrepancies, taking into account the five percent experimental uncertainties

Bifurcation	u	Theory	Experiment	|Diff.|	Max. Diff.
Hopf	u_H	8.40	8.04 ± 5 percent	4 percent	9 percent
Period doubling	u_{pd}	8.63–8.94	8.43 ± 5 percent	2–6 percent	11 percent
Chaos	u_{ch}	8.68–8.97	8.72 ± 5 percent	0.5–3 percent	8 percent

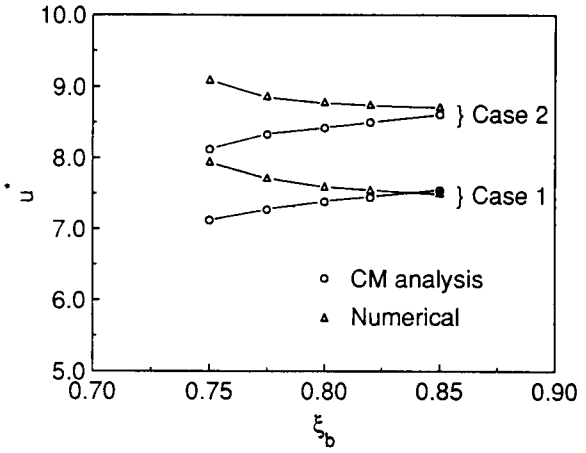

Fig. 6 The critical flow velocity, u^*, for instability of the limit cycle for a cubic spring, $\kappa = 100$, $\alpha = 0.005$ and Case 1: $\beta = 0.2$, $\gamma = 10$; Case 2: $\beta = 0.21$, $\gamma = 26.76$

The calculation was performed by using a MACSYMA computer algebra program (Rand and Armbruster, 1987) which accomplished the foregoing strategy as follows (the step numbers correspond to the numbers in the strategy in the previous paragraph):

1 An eigenanalysis is performed on the linearized equations at $u = u_H$ corresponding to the Hopf bifurcation, and thereafter define $\mu = u - u_H$. The variables in the nonlinear equations are changed, based on the eigencoordinates in the step above. Let y_1, y_2 be the eigencoordinates associated with purely imaginary eigenvalues, while y_3, y_4 correspond to those with negative real parts. The transformed equations are of the form

$$\dot{y}_i = F_i(y_1, y_2, y_3, y_4; \mu), \quad i = 1,2,3,4. \tag{8}$$

A center manifold (CM) is sought in the form of a power series,

$$\begin{aligned} y_3 &= a_1 y_1^3 + a_2 y_1^2 y_2 + a_3 y_1 y_2^2 + a_4 y_2^3 + a_5 \mu y_1 + a_6 \mu y_2, \\ y_4 &= b_1 y_1^3 + b_2 y_1^2 y_2 + b_3 y_1 y_2^2 + b_4 y_2^3 + b_5 \mu y_1 + b_6 \mu y_2. \end{aligned} \tag{9}$$

The actual computation has been automated (Rand and Armbruster, 1987). It consists of substituting (9) into (8) and determining the coefficients a_i and b_i by requiring that the y_3 and y_4 equations be identically satisfied (hence, the CM is an invariant surface).

2 Equations (9) are then substituted into (8) for $i = 1, 2$, giving the flow on the center manifold, in the form $\dot{y}_1 = G_1(y_1, y_2; \mu)$, $\dot{y}_2 = G_2(y_1, y_2; \mu)$. Then a perturbation method, in this case normal forms, is utilized (Rand and Armbruster, 1987) to obtain an approximate solution to the limit cycle in these equations, which will be of the form $y_1 = H_1(t;\mu)$, $y_2 = H_2(t;\mu)$.

3 To study the stability of the limit cycle $y_i = H_i(t;\mu)$, $i = 1,2$, perturbations are introduced away from the limit cycle along the directions y_3 and y_4 by introducing $y_3 = \bar{y}_3 + \zeta_3$, $y_4 = \bar{y}_4 + \zeta_4$, where $\bar{y}_3$ and $\bar{y}_4$ are given by equations (9). The resulting equations for ζ_3 and ζ_4 are

$$\frac{d}{dt}\begin{Bmatrix}\zeta_3\\ \zeta_4\end{Bmatrix} = \begin{bmatrix} \frac{\partial F_3}{\partial y_3} & \frac{\partial F_3}{\partial y_4} \\ \frac{\partial F_4}{\partial y_3} & \frac{\partial F_4}{\partial y_4} \end{bmatrix} \begin{Bmatrix}\zeta_3\\ \zeta_4\end{Bmatrix} \equiv [A(t;\mu)] \begin{Bmatrix}\zeta_3\\ \zeta_4\end{Bmatrix}, \tag{10}$$

where the elements of the $[A(t;\mu)]$ matrix are periodic (which results from the periodicity of the limit cycle). Then, numerical integration of (10) and Floquet theory are used to determine u^*, the smallest value of u for which instability results; from the foregoing sections it is known that this instability is associated with a pitchfork bifurcation.

An important restriction of the foregoing calculation procedure is that the original set of equations, and hence (8), be wholly analytic. In the formulation of equation (3) for the restraint stiffness, however, there is a discontinuity at $\eta = \eta_{bn}$. It is therefore necessary that calculations be confined to those of the earlier analytical model in which an analytic form of restraint stiffness was utilized: $f(\eta) = \kappa\eta^3$; in fact, one of the reasons for introducing this formulation in the earlier studies was so as to allow analysis as well as the computation of Lyapunov exponents.

The results of two sets of calculations are presented in Fig. 6 for systems with parameters as given in the caption. The variable parameter has arbitrarily been chosen to be the restraint location ξ_b. It is seen that with increasing ξ_b agreement between the values of u^* obtained by the center-manifold calculation and by numerical integration improves. The discrepancy between them, however, is in all cases less than 11 percent. This is remarkable, considering that the center manifold calculation involves neglecting terms of order μ^2 and that $\mu(=u-u_H)$, is not so small; e.g., for Case 1, $\xi_b = 0.82$, $u_H = 6.27$, and $u^* = 7.57$, so that $\mu = 1.30$ ($\mu/u_H = 0.21$).

For this analytical model ($f(\eta) = \kappa\eta^3$), the convergence of the critical flow velocities for the pitchfork and period doubling bifurcations and for chaos was also studied with an increasing number of degrees-of-freedom, N; it was found to be quite similar to those in the foregoing sections. The same may be said for the bifurcation diagrams.

7 Conclusion

The main contributions of this paper are three. First, a refined analytical model of the dynamical system was elaborated, to bring it closer to the experimental system than previous attempts, yet retaining its essential simplicity. Furthermore, by utilizing higher-dimensional models than heretofore ($N > 2$), it was for the first time possible to conduct numerical calculations with all parameters matching the experimental ones, without running into any difficulties of convergence of the solution. At the same time, by increasing the number of degrees-of-freedom (N) of the model, it was possible to demonstrate convergence of the results for $N = 4$ or 5 (for all three proposed representations for the restraint stiffness), in terms of the thresholds of pitchfork and period doubling bifurcations. This result agrees well with fractal dimension calculations on the experimental oscillation signal (Païdoussis et al., 1991), giving a fractal dimension of 3.2 in the chaotic regime. This suggests that while two-degree-of-freedom modeling is the bare minimum, as many as four or even five degrees-of-freedom may be necessary for an analytical model to capture the essential dynamics of the system.

The second important contribution of this paper lies in the *quantitative* comparison of theory to experiment. It is not surprising that the dynamical behavior was found to be in good *qualitative* agreement with observation, since simpler, lower-dimensional ($N = 2$) versions of the analytical model achieved as much (Païdoussis and Moon, 1988; Païdoussis et al., 1989, 1991). However, in this paper it has been shown that there is excellent quantitative agreement between theory and experiment as well, in terms of the Hopf and first period doubling bifurcation thresholds and of the onset of chaos: Discrepancies are of the order of five percent (or ten percent when experimental uncertainty margins are included).

The third item of interest in this paper concerns an analytical study of the stability of the limit cycle which emerges via the Hopf bifurcation. This was done by means of center manifold computations, with the aid of symbolic manipulation. Agreement with numerical results for the critical u at which stability is lost was found to be within 11 percent for a range of parameters tested, which is quite reasonable considering that the interval Δu between the Hopf and pitchfork bifurcation (which destroys the stability of the limit cycle) is not very small.

Acknowledgments

The authors gratefully acknowledge the support to this research by the Natural Sciences and Engineering Research Council of Canada and Le Fonds FCAR of Québec.

References

Axisa, F., Antunes, J., and Villard, B., 1988, "Overview of the Numerical Methods for Predicting Flow-Induced Vibration," ASME *Journal of Pressure Vessel Technology,* Vol. 110, pp. 6–14.

Gregory, R. W., and Païdoussis, M. P., 1966, "Unstable Oscillation of Tubular Cantilevers Conveying Fluid. I. Theory; II. Experiments," *Proceedings of the Royal Society London,* Vol. A293, pp. 512–527 and 528–542.

Holmes, P. J., 1977, "Bifurcations to Divergence and Flutter in Flow-Induced Oscillations: A Finite-Dimensional Analysis," *Journal of Sound and Vibration,* Vol. 53, pp. 471–503.

Hunt, K. H., and Crossley, F. R. E., 1975, "Coefficient of Restitution Interpreted as Damping in Vibroimpact," ASME JOURNAL OF APPLIED MECHANICS, Vol. 42, pp. 440–445.

Moon, F. C., 1987, *Chaotic Vibrations: An Introduction for Applied Scientists and Engineers,* John Wiley and Sons, New York.

Moon, F. C., 1988, "Chaotic Vibrations of a Magnet Near a Superconductor," *Physics Letters A,* Vol. 132, pp. 249–252.

Moon, F. C., and Li, G. X., 1990, "Experimental Study of Chaotic Vibrations in a Pin-Jointed Space Truss Structure," *AIAA Journal,* Vol. 28, pp. 915–921.

Païdoussis, M. P., 1970, "Dynamics of Tubular Cantilevers Conveying Fluid," *Journal of Mechanical Engineering Science,* Vol. 12, pp. 85–103.

Païdoussis, M. P., 1987, "Flow-Induced Instabilities of Cylindrical Structures," *Applied Mechanics Reviews,* Vol. 40, pp. 163–175.

Païdoussis, M. P., Cusumano, J. P., and Copeland, G. S., 1991, "Low-Dimensional Chaos in a Flexible Tube Conveying Fluid," ASME JOURNAL OF APPLIED MECHANICS, accepted for publication.

Païdoussis, M. P., and Issid, N. T., 1974, "Dynamic Stability of Pipes Conveying Fluid," *Journal of Sound and Vibration,* Vol. 33, pp. 267–294.

Païdoussis, M. P., Li, G. X., and Moon, F. C., 1989, "Chaotic Oscillations of the Autonomous System of a Constrained Pipe Conveying Fluid," *Journal of Sound and Vibration,* Vol. 135, pp. 1–19.

Païdoussis, M. P., and Moon, F. C., 1988, "Nonlinear and Chaotic Fluidelastic Vibrations of a Flexible Pipe Conveying Fluid," *Journal of Fluids and Structures,* Vol. 2, pp. 567–591.

Rand, R. H., 1989, "Analytical Approximations for Period-Doubling Following a Hopf Bifurcation," *Mechanics Research Communications,* Vol. 16, pp. 117–123.

Rand, R. H., and Armbruster, D., 1987, *Perturbation Methods, Bifurcation Theory and Computer Algebra,* Springer-Verlag, New York.

Tang, D. M., and Dowell, E. H., 1988, "Chaotic Oscillations of a Cantilevered Pipe Conveying Fluid," *Journal of Fluids and Structures,* Vol. 2, pp. 263–283.

Tousi, S., and Bajaj, A. K., 1985, "Period-Doubling Bifurcations and Modulated Motions in Forced Mechanical Systems," ASME JOURNAL OF APPLIED MECHANICS, Vol. 57, pp. 446–452.